THE EMERGING ERA OF VISIONARY COMPOSITES BY PLANT-GROWN MATRIX AND REINFORCING FIBRES: THE CELLULAR ADHESION

Mikko, Kanerva[a], Olli, Orell[a], Jarmo, Laakso[a], Alexandros, Prapavesis[b], Aart-Willem, van Vuure[b], Vladimir, Yudin[c], Ari-Pekka, Mähönen[d], Yrjö, Helariutta[d]

a: Tampere University, Engineering and Natural Sciences, Finland – mikko.kanerva@tuni.fi
b: KU Leuven, Department of Materials Engineering (MTM), Belgium
c: Institute of Macromolecular Compounds (IMC), Russian Federation
d: Helsinki University, Viikki Plant Science Centre (ViPS), Finland

Abstract: *The truly sustainable future with engineering materials will require completely new ways of creating materials. A significant part of emissions and energy consumption originates due to the processing of materials for various products, especially in the case of advanced composites. The more circular economy and recycling is to be applied, the more emphasis must be put on the processing of materials. In nature, the 'processes' of synthesis and material circulation are completely sustainable. This work includes actual field trials that were started during the year 2018 – aiming to the studies about the generation of fibre-reinforced visionary composites with the help of natural adhesion and cellular growth in pine trees.*

Keywords: bio-inspired; tree surgery; adhesion; cell proliferation, implantation

1. Introduction

It is not difficult to give reasons for why we should change the way our products, the materials in them, are produced nowadays. The global concentration of CO2 and the growth of its increase has only accelerated during the recent decades [1] – noting that CO2 emissions are regarded as one of the main parameters used to compute any (human) process-induced impact on the climate change. The reported values are already beyond the limits that could have been fought down – proper 'safeguarding' would have allowed to save the global economy [2, 3]. Similar large increases in the CO2 concentration of atmosphere, in the Earth's history, have only been related to total ecological phase changes along with the climate in the planet's history during tens of millions of years [4]. Most of the human's energy consumption is related to processing of Earth resources into different products as well as transporting the raw materials and products from a place to another all over the globe [5]. The activity related to various processes by humanity has long led to significant appropriation on the scale of the Earth ecosystem [6]. Only completely different processes of making materials and products for human needs can be sustained in the future. For future materials, humans must learn to adapt with the synthesis, or conversion, of matter in nature.

Purely from the point of view of engineering, wood – after harvesting and dehydration – has good static strength (e.g., 173 MPa for mararie, *Karrabina benthamiana*) and Young's modulus (e.g., 19 GPa for yellowwood, *Cladrastis kentukea*). These values are significantly higher than those of any polymeric matrix used in the advanced fibre reinforced composites today. Recently, Kyoto University and a company launched a development project about the use of wood materials in satellite enclosures to prevent waste accumulation in Earth orbit [7]. Plywood has

  doi:10.5075/epfl-298799_978-2-9701614-0-0

been used in primary and secondary load-carrying structures in aircraft for decades. Wood and plant stems in general are anisotropic, in terms of the structure and (mechanical) properties, and this suggests that the functional properties as well as mechanics can theoretically be tailored in the final material system [8]. It is important to note that anisotropy is basically the reason why modern fibre reinforced polymer composites (FRPCs) can be much further optimized per application than any isotropic alloy or amorphous material. Interestingly, over the recent few tens of years, scientists have pursued to improve the fibre-matrix interphases in fibrous composites [9]. In this study, the efforts aim to hierarchical, controlled anisotropy in future visionary FRPCs with nature. It is well known that tailored interphases in fibrous composites with multi-scale structuring can give engineering materials not only targeted static mechanical performance but improved fatigue and dynamic response, to be exploited in the design of high-tech products [10]. Wood structure is inherently hierarchical, anisotropic, and specifically controlled for each stress condition by trees themselves [11].

2. Experimental

2.1 Materials

This study was carried out with pine (*Pinus sylvestris*) and synthetic fibres for selected functionalities and as implant parts. In general, of all plants, pine trees naturally exist on all the continents of the Northern Hemisphere. They are available in massive amounts without any industrial cultivation and exist nearby local engineering industries. Therefore, pine tree-based materials have the potential to be used sustainably without long-distance transportation between different continents. Additionally, conifer forests are the largest terrestrial carbon sink. Pine trees have been studied for decades and there are large amounts of scientific literature available about the tissue structure, growth, evolution, and extractives (resins) of various pine trees, making this tree genus a scientifically rather well-defined organism.

The four different fibres representing the implant materials were: 1) carbon (carbon) fibres with the minimum surface finish (Elur®-p-0.08, by Argon LLC, provided by the Institute of Macromolecular Compounds (IMC)), 2) ECR (electrical/ chemical resistance) glass (glass) fibres (provided by Kevra Oy, Finland), 3) high-density polyethylene (PE) fibres (PE melt-spun as described in the previous work [12]) using CG9620 granulate (Borealis Polymers, Austria), and 4) diamond-like carbon (DLC) coated aramid fibres (coating [10] by DIARC® Bindo, by Oerlikon Balzers Coating, Finland) of grade Twaron® 2200 (by Teijin, Japan). Carbon fibre has the greatest potential to improve the stiffness and strength for any alive or post-cut wood-carbon fibre composite as well as it conducts heat and electricity.

For adjusting the compatibility between the cell proliferation and fibre surfaces, pine gum rosin (Forchem, Finland) was used as treatment. The treatment (i.e., dilute solution of dissolved rosin and acetone) was applied by dipping. Whenever tree surface (bark) gets broken, a path is formed via wounds for insects and fungi to attack the internal tree tissue. Therefore, the surface treatments with rosin targeted to ensure healthy, well-grown wounds. The rosin treatment was studied for carbon (carbon-R) and glass fibres (glass-R) series.

  doi:10.5075/epfl-298799_978-2-9701614-0-0

2.2 Outdoor field trial with tree surgery

The growth-integrated composites were grown in Finnish forest using pine (*P. Sylvestris*). The alive meristem cells within the vascular cambium were reached from U-cuts from the bark layer (see Fig. 2 a). Each implant material was studied for two different implantation techniques: I) upward U-cut with half of fibre bundle left outside tree surface, for later characterization with a pull-out method, and II) upward U-cut with full embedment. Each tree, and each cut (manually done by using a sterilized surgeon scalpel Cutfix®, B. Braun Melsungen), was in details identified by the cut length, cut location (direction, height, number of branch fork), and tree dimeter at the surgery location prior implantation. The length of the implant (fibre) samples was 20 mm for full embedment (U-cut length 22-40 mm) giving a length to diameter ratio of ≈1000 (fibre diameter for the different fibres 10-80 µm). All the implanted tree individuals were grown inside a 100 sqm plantation with as similar lighting, weather, and nutrients (soil type) as possible for the outdoor forest-based field trial. The wounds (at implantations) were treated with wound wax (080E1, Neko) and wrapped by tar-treated fabric tape (batch 10.04.002, Finland) as is a typical wound treatment. The tape was removed after two months of tree growth to allow normal bark formation. The healing (proliferation) period (during the years 2018-2019) was in total 17.5 months (i.e., two radial growth terms for pine). Sections were extracted from the pine stems and cut pieces were dehydrated slowly in standard room conditions (21±1 °C, 65% RH) over 12 months. The final pieces included control pieces of un-intervened wood and the growth-integrated pieces.

2.3 Mechanical testing

The dehydrated wood pieces were fine-cut and polished into specimens for three-point bending testing to study increases in flexural strength (28 mm × 8 mm × 8 mm, length × width × height). A three-point bending test fixture was used for flexural testing with a span length of 22 mm, loading pin diameter of 10 mm, and support pin(s) diameter of 5 mm. A universal test machine was used to generate the compressive load (5967, Instron, operated at a 1.0 mm/min test rate). Each specimen was loaded up to the failure load. Peak force and failure mode were recorded. The flexural (longitudinal) strength was defined for the failure with Eq. (1):

$$\sigma_u = \frac{3 \cdot F_u \cdot s}{2 \cdot w \cdot h^2} \tag{1}$$

where F_u is the peak force during a test, s is the support pin span, w is the test specimen's width, and h is the test specimen's height. Flexural strength was calculated for each specimen with specimen's individual exact dimensions. Three pure wooden (no fibres) specimens (see Fig. 2 b) were tested to determine the average reference strength (σ_{ref}). The effect of the grown-integration of fibres was studied via the difference between the flexural strength of fibre-integrated specimen and reference strength ($\Delta\sigma_u$). The conditions during the tests were recorded (20.5 °C, 23% RH).

A new method was generated to pull out and test for adhesion the specimens with growth-integrated glass fibres. In the pull-out testing, fibres or a set of fibres (bundle) were pulled out of the matrix amid (here wood or combination of wood and rosin). The higher is the force (stress) needed to pull, the higher is the interfacial adhesion reflected by the test. The designed test setup is illustrated in Fig. 2 c. A universal test machine was used to generate the load (5967, Instron, operated at a 1.0 mm/min test rate, 5.0 N miniature load cell). To grip a fibre or bundle,

  doi:10.5075/epfl-298799_978-2-9701614-0-0

thin veneer tabs were used; fibre (bundle) was adhesively (using polyvinyl acetate glue) connected between two tabbing pieces.

a) 

b) 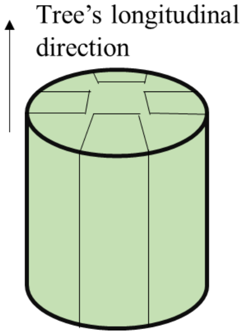

c) 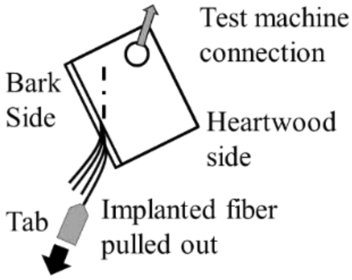

Figure 2. a) U-cut for fibre integration (DLC series in the image); b) pieces extracted from pine tree stem for flexural testing; c) the pull-out test method concept.

2.4 Microscopy and characterization

Field emission (FESEM) scanning electron microscopy (ULTRAplus, Zeiss) was used to study the integration of fibres amid the grown cellular wood structure. Cross-sectional ion polishing (CSP) was used to reveal the ultracellular structure of the adhered cells amidst the fibres and these samples were imaged by FESEM. Compositional analysis (x-ray energy dispersive spectroscopy, EDS) was used to observe fibres.

The fibre integration and fracture formations in the flexural specimens were studied with the help of 3D imaging with X-ray Computed Tomography (XCT) using TESCAN UniTOM HR scanner, equipped with a 160 kV/25 W microfocus & nanofocus X-ray tube, with a tungsten reflection target and a detector of 2916 x 2280 pixels, with a 50 µm pixel pitch. The source voltage and power were set to 55 kV and 0.8 W. Based on the source-to-object distance two voxels size (VS) magnifications were acquired; a) a 10 µm VS scan for the overall inspection of the specimen and b) high resolution scans of 1 µm VS in selected volumes of interest. In total 2600 radiographic projections were acquired over a 360° sample rotation, each with an exposure time of 1200 ms and frame averaging set to 5 to reduce the random noise, resulting in acquisition times of 260 min per scan. Thereafter, cross-sectional reconstruction to tomographic slices performed on the acquired radiographic projections by applying a filter back-projection algorithm in the TESCAN reconstruction software Panthera. Image analysis and 3D visualization of the scans was performed in Avizo 3D v 2021.1 (ThermoFisher)

2.5 Finite element analysis

The pull-out test method was analyzed using simulation on the finite element (FE) basis. The modelling and computations were carried out in ABAQUS (Standard) (2021). The part geometries included 3D models of a wooden part (2 mm × 1 mm × 0.4 mm) and fibre (ø 18 µm, length 4.5 mm). Rigid contacts (tie) were used between the wood and fibre parts. Wood was modelled to be an anisotropic elastic body (moduli $9.7\cdot10^{-3}$ N/µm^2, $5.8\cdot10^{-4}$ N/µm^2, $5.8\cdot10^{-4}$ N/µm^2, shear moduli $3.6\cdot10^{-3}$ N/µm^2, $3.6\cdot10^{-3}$ N/µm^2, $2.8\cdot10^{-4}$ N/µm^2, Poisson's ratios 0.33, 0.33, 0.02, in a Cartesian coordinate system XYZ, respectively, with X-axis matching with the longitudinal (upwards) tree growth [13]). The fibre part was modelled to be an isotropic body (glass, 0.07 N/µm^2, Poisson's ratio 0.3). The fibre was divided into three parts: the free end (50 µm) of the fibre was rigid for a clamped boundary condition, and the portion inside wood

  doi:10.5075/epfl-298799_978-2-9701614-0-0

was divided into two portions (fibre and a 0.5 mm-internal portion). The internal portion was modelled either 1) glass fibre, or 2) softer, rosin-imitating material ($1 \cdot 10^{-6}$ N/μm^2, Poisson's ratio 0.3). The fibre part was integrated into the wood part at a pull-out angle of 15°. Linear hybrid tetras (C3D10) were used for meshing (nominal size at the interfaces 8 μm). The total mesh included 133 178 elements. The simulation of the pull-out test was run for a constant pull-out force of 0.1 N (point load at the bottom of the wood part). It was estimated that, in a typical real test, there are in average 10 fibres pulled out simultaneously for an experimental peak of ≈1 N.

3. Results and analysis

3.1 Wound healing and cellular structure

The total tree mass was measured at the time of cutting (after the field trial): 8.3 kg, 7.2 kg, 9.1 kg, 6.3 kg, for the trees used in grow-integration of PE, DLC, glass, carbon series, respectively. The increase of diameter at the implantation location was: 38 % (15.8 mm), 49 % (20.6 mm), 58 % (25 mm), 37 % (14.7 mm) for PE, DLC, glass, carbon series, respectively.

The wounds healed so that the U-cut was grown back over all its edges (Fig. 3 a) for all the glass and carbon series. For PE and DLC series, the wounds did not heal well and, especially for the partly embedded fibres, the U-cut did not grow back but was left partly open. For all glass and carbon series, the fibres were adhered, i.e., grown several millimeters inside the wood. The intervention led to secretion of rosin by the tree, as was revealed by the FESEM imaging (Fig. 3 b). For the carbon series where no rosin-treatment was applied, the rosin secretion was significant and visually observable after breakage of the specimen within flexural testing. For the rosin-treated carbon fibres, the secreted rosin was less but clearly visible in XCT analysis on micro-scale (Fig. 4 a-b).

a) 

b) 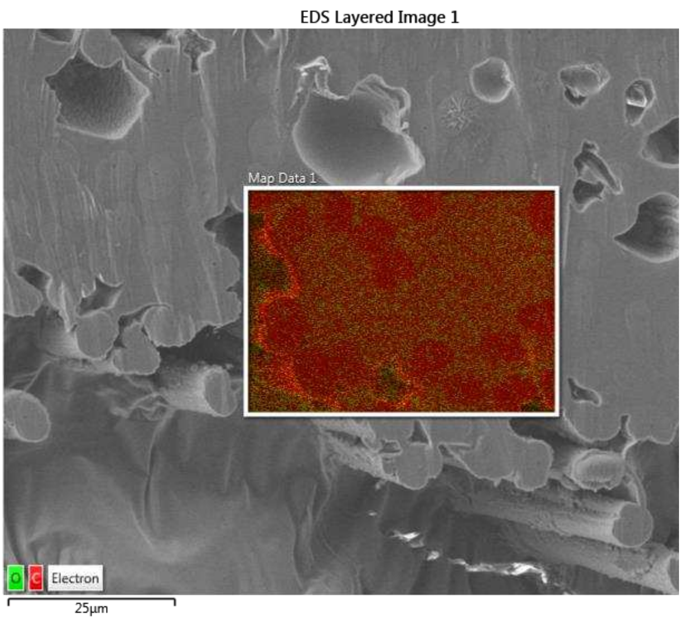

Figure 3. a) Wound healing on pine stem for carbon fibres (without rosin treatment) fully implanted. b) FESEM and related EDS analysis of carbon-series specimen.

a) 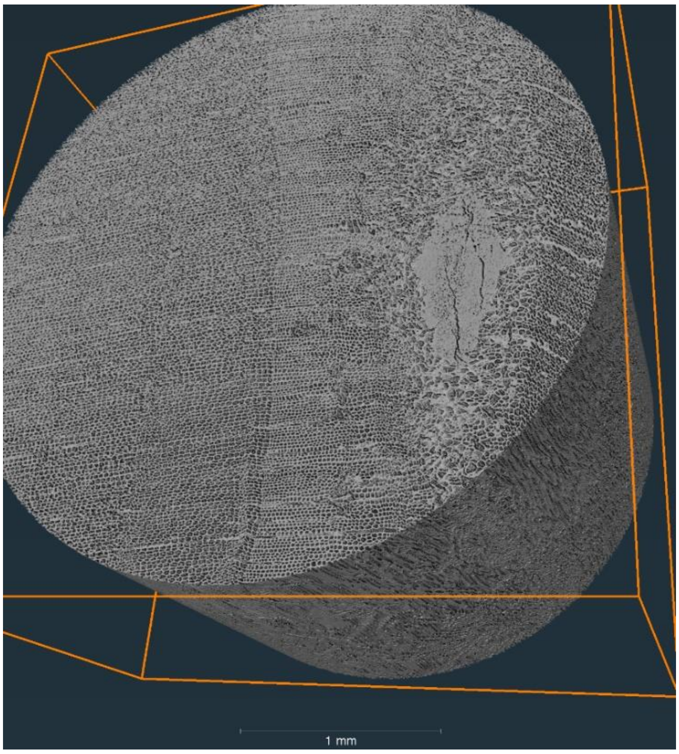 b) 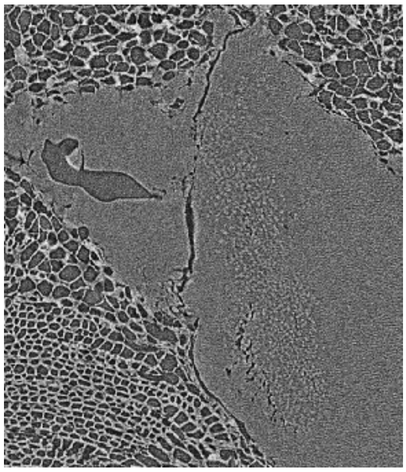

Figure 4. a) 3D analysis of the carbon fibres inside the wood piece based on the XCT analysis; b) 2D cross-section by the XCT analysis of carbon fibres, surrounded by secreted rosin.

3.2 Improvements of mechanical performance

The results of the flexural testing are shown in Fig. 5. a, and the results of pull-out tests in Fig. 5 b. The flexural strength was improved by fibre-integration for all the series except for carbon fibres without the rosin surface treatment. The rosin treatment improved the flexural strength for the carbon fibre integration by 32 % and for the glass fibre integration by 3 %. The fibre integration with rosin treatment, compared to pure wood, increased the strength by 8 % for the carbon series (carbon-R) and 15 % for the glass series (glass-R). Fibre volume fraction was estimated based on cross-sectional areas of specimen ($64 \cdot 10^{-6}$ m^2) and fibres ($\pi r^2 = 80 \cdot 10^{-12}$ m^2; for 100 fibres in a bundle yields $80 \cdot 10^{-10}$ m^2) the longitudinal dimension being essentially equal (specimen's length). This estimation gives a fibre volume fraction of 0.1-0.2 ‰ in the fibre-integrated samples. It should be noted that the flexural strength was significantly increased for the PE and DLC series although the implanted fibres were not well integrated (unsuccessful healing). This indicates that the surgery for implantation is a type of intervention that leads to wound tissue of a higher strength. In other words, the improvements of flexural strength in Fig. 5 a are not only due to the implanted fibres but also due to the changes in the cell structure of wood (see variation in Fig. 4 a) compared to the non-intervened wood of reference specimens.

Significant improvements in (flexural) strength would require good adhesion between the implanted fibres and the proliferated cell tissue amid. However, there are no test methods for measuring the mechanical adhesion forces for wood-fibre materials with grown adhesion. Therefore, a pull-out method was developed and studied. The results of pull-out testing for the glass series are shown in Fig. 5 b. It was found that the peak force can be related to various failure modes, such as partial pull-out and fibre (bundle) breakage. Further research is needed to improve and analyze the pull-out method in detail.

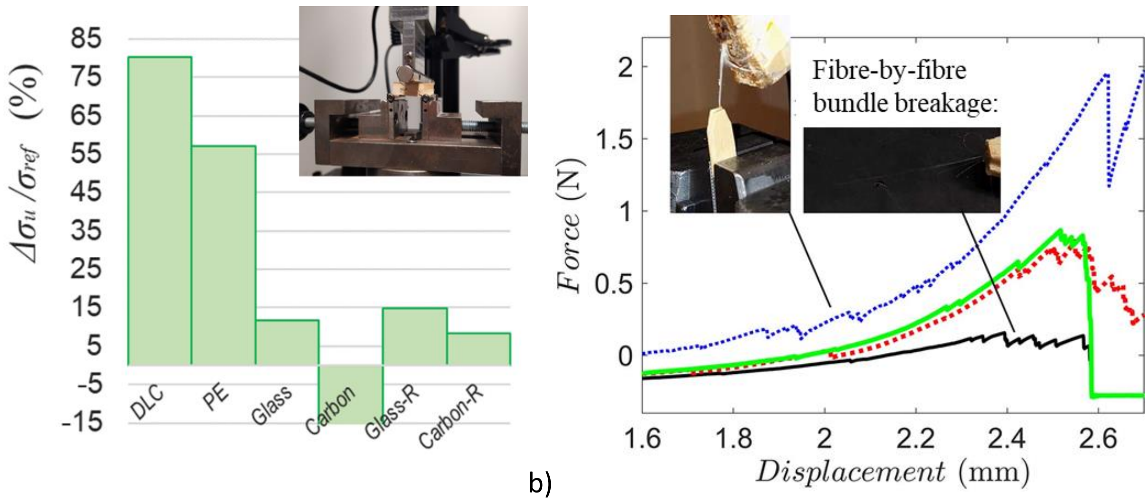

Figure 5. a) Change in flexural strength due to grown-integrated fibres;
b) the force-displacement performance of glass fibres pulled out from wood.

3.3 Numerical analysis of the pull-out test method

The von Mises maps are shown in Fig. 6. The stresses at the fibre-wood interface were carried approximately by a portion up to 1 mm of length (inside the wood part). It should be noted that (unhomogenized) real cell structure of wood would allow local yield and the stress-carrying length could be longer, yet the effect is anticipated up to a factor of two. Therefore, in the real test, fibre pull-out clearly requires breakage of fibre near the specimen surface or crack growth along the fibre-wood interface because the fibres were grown to adhesion along a length of approximately 20 mm of fibre inside the wood.

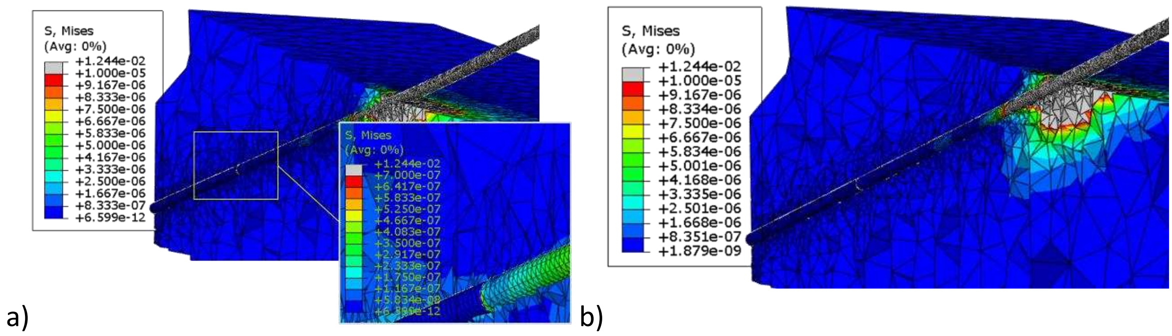

Figure 6. FE analysis results for simulated fibre pull-out tests at a peak force of 0.1 N: a) fibre integrated at a depth of 0.7 mm followed by a rosin-filled cavity; b) fibre integrated throughout (1.2 mm). A half of the wood part have been removed from the visualization for clarity. In the stress legends, the unit of stress is N/μm^2, e.g., $1\cdot10^{-5}$ *N/μm*^{2} = 10 *MPa*.

4. Conclusions

This work confirmed that making advanced composites can be done in close collaboration with alive plants. Different fibres were implanted into alive pine tree stem and the performance was studied after extraction of composite pieces formed by the fibres and grown cellular tissue. The healed tissue is irregular and affects the composite properties in addition to the fibres and when compared to the intact wood around the integration volume.

Nowadays, human civilization establishes its ‘intelligence’ in terms of war and disregard of nature. A change in the mindset is necessary to focus altogether on collaborative living, produce and use physical matter in a harmony with nature – right now and in future.

Acknowledgements

This study made use of the Microscopy Center of Tampere University. The authors want to thank J. Alonso-Serra (RDP-INRAE-ENS de Lyon, France) for collaboration.

5. References

1. Dlugokencky E, Tans P. Global Annual Mean Dioxide Growth Rate. NOAA Research/GML. cited: March 2022. https://www.esrl.noaa.gov/gmd/ccgg/trends/gl_gr.html
2. Steffen W, Broadgate W, Deutsch L, Gaffney O, Ludwig C. The trajectory of the Anthropocene: The Great Acceleration. The Anthropocene Review 2015; 2: 81-98.
3. Figueres C, Schellnhuber HJ, Whiteman G, Rockström J, Hobley A, Rahmstorf S. Three years to safeguard our climate. Nature 2017; 546: 593-595.
4. Anagnostou E, John EH, Edgar KM, Foster GL, Ridgwell A, et al. Changing atmospheric CO2 concentration was the primary driver of early Cenozoic climate. Nature 2016; 533: 380-384.
5. Haberl H, Erb KH, Krausmann F, Gaube V, Bondeau A, et al. Quantifying and mapping the human appropriation of net primary production in earth's terrestrial ecosystems. PNAS 2017; 104: 31
6. World Energy Outlook 2019. Flagship report — November 2019. IEA. 2019. Cited: March 2020. https://www.iea.org/reports/world-energy-outlook-2019
7. Harper J. Japan developing wooden satellites to cut space junk. BBC News. 2020. Cited: March 2022. https://www.bbc.com/news/business-55463366
8. Zhongsen Zhang, Shenming Cai, Yan Li, Zhen Wang, Yu Long, et al. High performances of plant fiber reinforced composites—A new insight from hierarchical microstructures. Composites Science and Technology 2020; 194: 108151.
9. Qian H, Greenhalgh ES, Shaffer MSP, Bismarck A. Carbon nanotube-based hierarchical composites: a review. Journal of Materials Chemistry 2010; 20: 4751-4762.
10. Kanerva M, Korkiakoski S, Lahtonen K, Jokinen J, Sarlin E, et al. DLC-treated aramid-fibre composites: Tailoring nanoscale-coating for macroscale performance. Composites Science and Technology 2019; 171: 62-69.
11. Alonso-Serra J, Shi X, Peaucelle A, Rastas P, Bourdon M, et al. The ELIMÄKI Locus is Required for Vertical Proprioception in Birch Trees. 2019. Available at SSRN: https://ssrn.com/abstract=3444593 or http://dx.doi.org/10.2139/ssrn.3444593
12. Kanerva M, Puolakka A, Takala TM, Elert AM, Mylläri V, et al. Antibacterial polymer fibres by rosin compounding and melt-spinning. Materials Today Communications 2019; 20: 100527
13. Green DW, Winandy JE, Kretschma DE. Mechanical Properties of Wood. Forest Products Laboratory. 1999. In: Wood handbook—Wood as an engineering material. Gen. Tech. Rep. FPL–GTR–113. Madison, WI: U.S. Department of Agriculture, Forest Service, Forest Products Laboratory.